GEOGRAPHICAL REPORTS
OF TOKYO METROPOLITAN UNIVERSITY 54 (2019) 11–22

AUTUMN RAINFALL INCREASING TREND IN SOUTH CENTRAL VIETNAM AND ITS ASSOCIATION WITH CHANGES IN VIETNAM'S EAST SEA SURFACE TEMPERATURE

Long TRINH-TUAN, Rakesh Teja KONDURU, Tomoshige INOUE, Thanh NGO-DUC[*] and Jun MATSUMOTO

Abstract Certain parts of Southeast Asia, such as central Vietnam, experience heavy rainfall in the boreal autumn from September to December (SOND). The 52-year SOND rainfall over Vietnam from 1961 to 2012 shows increasing trends over the south central region (SR). Along the central coastal regions and SR, SOND rainfall as well as heavy rainfall indices, such as the number of heavy rainfall days, have increased significantly since the late 1980s and early 1990s. In contrast, a decreasing trend is observed in stations located north of 17°N. Tropical cyclone-induced rainfall exhibits an increasing trend over the SR. The increasing trend of SOND rainfall is associated with the recent sea surface temperature (SST) warming after the late 1980s over the South Vietnam East Sea (SVES). Owing to the recent SST warming and grand La Niña-like pattern after the 1990s, the SVES surface temperature has increased by 0.8–1.2 °C over the period 1961–2012, leading to enhanced moisture flux convergence over the SR. Moreover, the SVES warming strengthens the anomalous northeasterly winds that affect the SR. Consequently, SR has become more prone to deep convection and heavy rainfall events.

Keywords: rainfall trend, sea surface temperature, heavy rainfall

1. Introduction

Rainfall variability significantly affects developing countries such as Vietnam, whose economy and sociology depend strongly on agriculture. In general, rainfall in Vietnam is dominated by the summer rainy season, which occurs from early May to mid-August and the autumn rainy season from mid-September to mid-December (Nguyen-Le *et al*. 2015). In most Asian monsoon regions, major rainfall is received during the boreal summer season, whereas rainfall in central Vietnam is concentrated during the boreal autumn to early winter (September to December, hereinafter SOND, Matsumoto 1997; Matsumoto *et al.* 2017). The SOND rainfall over central Vietnam occurs primarily due to tropical cyclone (TC) activities, the migration of the inter-tropical convergence zone

[*] Department of Space and Aeronautics, University of Science and Technology of Hanoi (USTH), Vietnam Academy of Science and Technology (VAST), Vietnam.

(ITCZ), and the northeast monsoon (Phan *et al.* 2009; Chen *et al.* 2015a, 2015b). Extreme rainfall sometimes occurs when these mentioned factors interact with the Truong Son mountain range (Fig.1a) as an orographic effect (Yen *et al.* 2011). Yokoi and Matsumoto (2008) investigated the synoptic-scale atmospheric conditions leading to a heavy rainfall in central Vietnam in early November 1999 and concluded that a northerly wind anomaly from the winter monsoon cold surge in the lower troposphere together with southerly wind anomaly over the adjacent sea was responsible for it. Wu *et al.* (2012) indicated that the heavy rainfall events that occurred over central Vietnam in early October of 2010 were associated with the westward-propagating synoptic-scale disturbances from the western Pacific, and the eastward propagation of a strong active phase of the Madden Julian Oscillation (MJO).

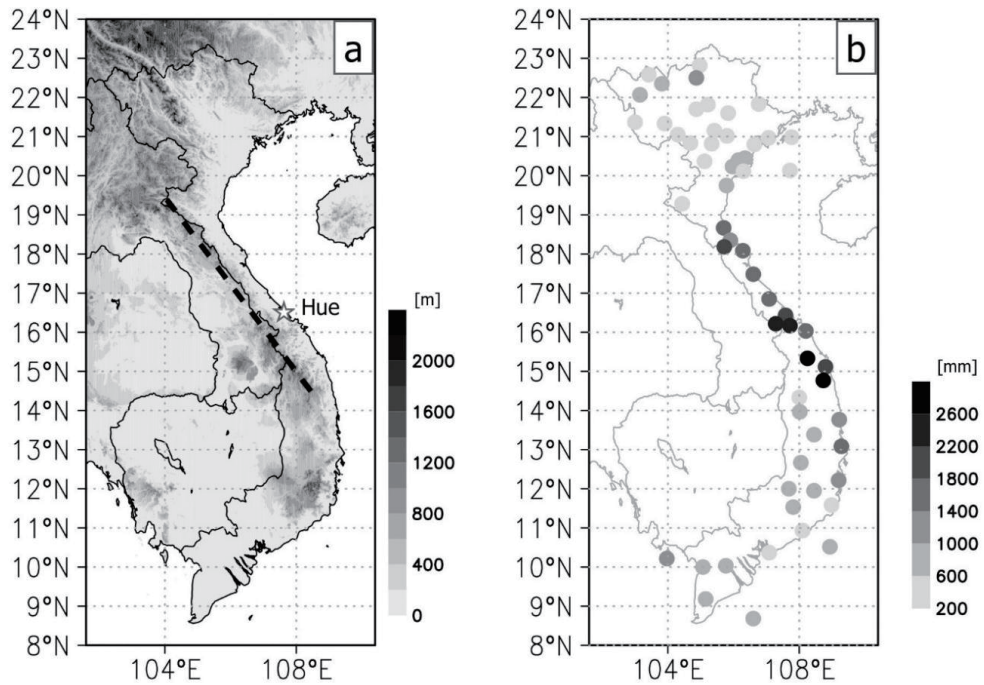

Fig. 1 (a) Topography of Vietnam. The broken line indicates the Truong Son Mountain Range. Star indicates Hue station (107.6°E, 16.4°N). (b) Climatological SOND rainfall averaged for the period 1961–2012 calculated based on data from 59 rain gauge stations in Vietnam.

As for rainfall variations over longer timescales, Endo *et al.* (2009) investigated trends in rainfall extremes in Southeast Asian countries from the 1950s to 2000s using extreme precipitation indices. They reported increasing trends in heavy precipitation over southern Vietnam, northern Myanmar, and some areas in the Philippines, and a decreasing trend in northern Vietnam. However, these extreme precipitation indices were only analyzed based on the annual computed values; therefore, it is important to determine whether the rainfall trend in a specific season is typical to the annual trend. Villafuerte and Matsumoto (2015) detected the increasing trend of both annual and autumnal

(October–December) maximum daily rainfall (Rx1day) in central Vietnam from 1951 to 2007 using the data from the Asian Precipitation – Highly-Resolved Observational Data Integration Towards Evaluation of the Water Resources (APHRODITE) project (Yatagai *et al.* 2012). They found that the trend of Rx1day was linked to the increasing global mean temperature.

The inter-annual variability of rainfall in Vietnam is affected by changes in the lower boundary such as sea surface temperature (SST), moisture transport, and large-scale circulations (Chen *et al.* 2012; Nguyen-Le and Matsumoto 2016). Yen *et al.* (2011) demonstrated that rainfall in October to November over central Vietnam is correlated well with SST anomalies over the equatorial eastern Pacific, which is associated with the El Niño-Southern Oscillations (ENSO). They indicated that the inter-annual rainfall variation over this region was primarily attributed to heavy rainfall events that occur approximately once every season. The impact of local SST on SOND rainfall has not been evaluated thus far. In particular, the local impact of the sea surface conditions over the Vietnam East Sea (VES) has not been examined in previous studies. Therefore, in the present study, we will investigate the long-term changes in SOND rainfall for the period of 1961–2012. Subsequently, the link between the changes in SOND rainfall and SST in the VES will be examined. Moreover, the associated changes in the atmospheric dynamics, and thermodynamic fields will be analyzed to establish their relationships with rainfall trends over Vietnam.

2. Data Sources and Methodology

Data sources

Daily and monthly rainfall from 1961 to 2012 were collected from 59 rain gauge stations (Fig. 1b) of the Vietnam Meteorology and Hydrology Administration (VNMHA), including 32 stations located to the north of 17°N (NR) and 27 stations to the south of 17°N (SR), and gridded dataset of the Global Precipitation Climatology Centre (GPCC; Schneider *et al.* 2015) from 1961 to 2012. In this study, we extracted and analyzed the data from stations that satisfy the following conditions: (1) more than 30 years of rainfall data existed; (2) SOND seasons with more than 10 years of missing data were not included for extreme index calculation. The quality of the rain gauge station data was verified using the five-sigma rule following Nguyen-Xuan *et al.* (2016).

Long-term changes in the large-scale circulation were investigated using a subset of the Japanese 55-year Reanalysis dataset (JRA-55; Kobayashi *et al.* 2015) produced by the Japan Meteorological Agency, namely the JRA-55 Conventional (JRA-55C; Kobayashi *et al.* 2014). The JRA-55C dataset is more homogeneous over a long period and unaffected by changes in historical satellite observing systems. Therefore, this dataset is suitable for studies of long-term climate variabilities. In the JRA-55C dataset, the daily data of zonal and meridional components of wind (*u, v*), specific humidity, air temperature, and geopotential height at multiple pressure levels were considered. To examine the long-term changes of TCs associated with the rainfall trends, the TC best track data provided by the Joint Typhoon Warning Center (JTWC) were used. The monthly data of Hadley Centre Sea Ice and SST version 1.1 (HadISST v1.1) (Rayner *et al.* 2003) with 0.5-degree grid resolution were used to study the SST change in the VES region. Additionally, the ocean heat flux and evaporation products were provided by the Woods Hole Oceanographic Institution Objectively Analyzed air–sea Fluxes (OAFlux) project (http://oaflux.whoi.edu). The National Oceanic and Atmospheric Administration daily outgoing longwave radiation (OLR), with a 2.5-degree grid resolution (Lee 2014), were

obtained for the period of 1974–2012 from https://www.esrl.noaa.gov/psd/.

Methodology

In this study, the trends of SOND rainfall (Pav) and extreme precipitation indices (PIs) (Table 1) including the number of rainy days (RR01), number of heavy rainfall days (R50 mm), and Rx1day, were investigated using the Kendall–Theil robust line method (Sen 1968, Granato 2006). Further, the trends of SST, winds, vertically integrated moisture flux convergence (VIMFC), and other meteorological variables were computed using the same method. To examine the statistical significance at the 5% level of the trend, we applied the non-parametric Mann–Kendall trend test (MK test; Kendall 1975).

Table 1 Definition of the precipitation indices (PIs) used in the study.

Index	Definition	Unit
Pav	Seasonal mean precipitation	mm day^{-1}
RR01	Seasonal rainy days when daily precipitation ≥ 1 mm	days
R50mm	Seasonal count of days when daily precipitation ≥ 50 mm	days
Rx1day	Seasonal maximum 1-day precipitation	mm

Moisture dynamics were computed using equations 1, 2, and 3. Equations 1 and 2 show the calculation for the vertically integrated moisture transport (VIMT) in the zonal (Q_u ; units = kg m^{-1} s^{-1}) and meridional (Q_v) directions, respectively.

$$Q_u = \frac{1}{g}\int_{p_{top}}^{p_{sfc}} uqdp, \tag{1}$$

$$Q_v = \frac{1}{g}\int_{p_{top}}^{p_{sfc}} vqdp, \tag{2}$$

where u and v are the zonal and meridional components of the wind, respectively; g is the acceleration owing to gravity (9.8 m s^{-2}); q is the specific humidity (kg kg^{-1}); p is the pressure; p_{top} and p_{sfc} are the pressures at the top and surface layers, respectively. The vertically integrated moisture flux convergence was calculated using equation 3 (VIMFC; units = kg kg^{-1}s^{-1}).

$$VIMFC = -\frac{1}{g}\left[dy\int_{p_{top}}^{p_{sfc}}\left(q\frac{\partial u}{\partial x}+u\frac{\partial q}{\partial x}\right)dp + dx\int_{p_{top}}^{p_{sfc}}\left(q\frac{\partial v}{\partial y}+v\frac{\partial q}{\partial y}\right)dp\right], \tag{3}$$

where VIMFC (Banacos and Schultz 2005) was computed for the vertical column of atmosphere from 1000 to 300 hPa.

3. Observed Trends in Rainfall during Boreal Autumn

The distribution of climatological SOND rainfall is represented using the rain gauge stations over Vietnam (Fig. 1b). As shown, along the coastal line between 12°N to 19°N, the SOND rainfall accumulation is generally greater than 1000 mm. In addition, the major autumn rainfall in central Vietnam is primarily produced by heavy rainfall associated with flood events (Chen *et al.* 2012). One of the record-breaking heavy rainfall spells in Vietnam occurred in the beginning of November 1999, which caused heavy flooding in the east coastal area in central Vietnam, in the area between 15.6°N to 16.7°N. In this event, the observed daily rainfall amount at the Hue station (Fig. 1a) was more than 1800 mm within 48 h (Yokoi and Matsumoto 2008).

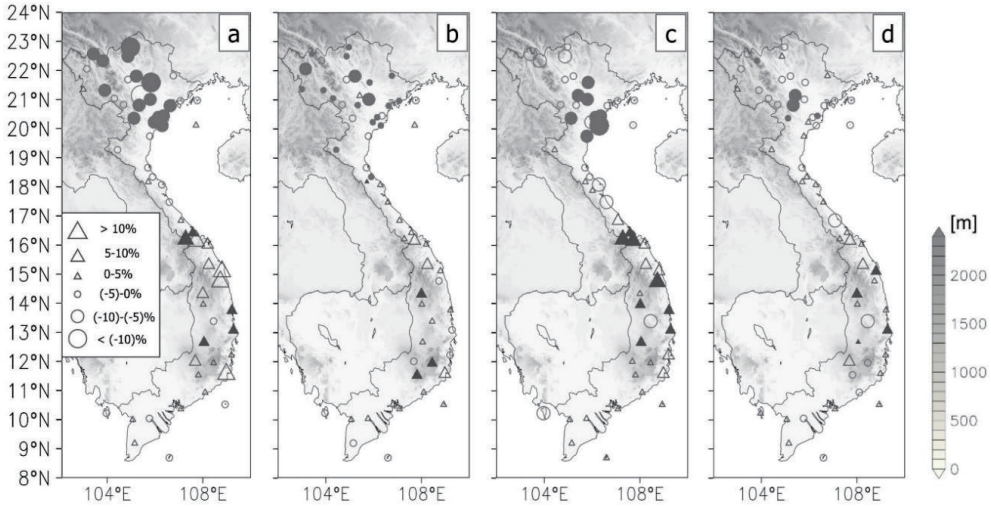

Fig. 2 Trends in (a) Pav, (b) RR01, (c) R50mm and (d) Rx1day. Trends are calculated as percentage variations with respect to the mean value per decade. Triangle (circle) symbols indicate an increasing (decreasing) trend. Solid symbol denotes statistical significance at 5% level.

The spatial distributions of PIs trends were plotted based on the station calculations (Fig. 2). In general, the opposite trends of PIs in NR and SR are clearly seen. In the northern region, significant decreasing trends in Pav are observed at 15 stations, with changing rates greater than 5% per decade. Meanwhile, over the SR, increasing trends are pronounced at 22 stations. It is worth noting that in the coastal region from 11°N to 17°N, most stations exhibit increasing rates larger than 5% per decade and 5 stations demonstrate a significant increase. Regarding the trends of PIs, in the northern region, the decreasing rates of RR01 and Rx1day are primarily less than 5% per decade. Meanwhile, R50mm's rate is greater than 5% at 14 stations. In contrast, R50mm in the SR tends to increase noticeably at 15 stations, with the rate exceeding 5%. Eight out of these 15 stations demonstrate a significant increase. The number of stations with significant increase in RR01 and Rx1day is less than those that demonstrate the same signal change in R50mm. The boundary of the contrasting rainfall trends between the northern and southern regions can be depicted around 17°N. This corresponds well with the results reported by Villafuerte and Matsumoto (2015), who found a

significant increase in Rx1day over south–central Vietnam in the season between October to December. To reveal the epochal difference, the latitudinal mean of SOND rainfall was displayed based on five-year running mean GPCC dataset for Vietnam land only (Fig. 3). It is clear that the location of the region of maximum rainfall remains around 15–17°N before 1986. After 1990, maximum rainfall tends to be intensified and its center occurs approximately 1° to 2° southward in latitude.

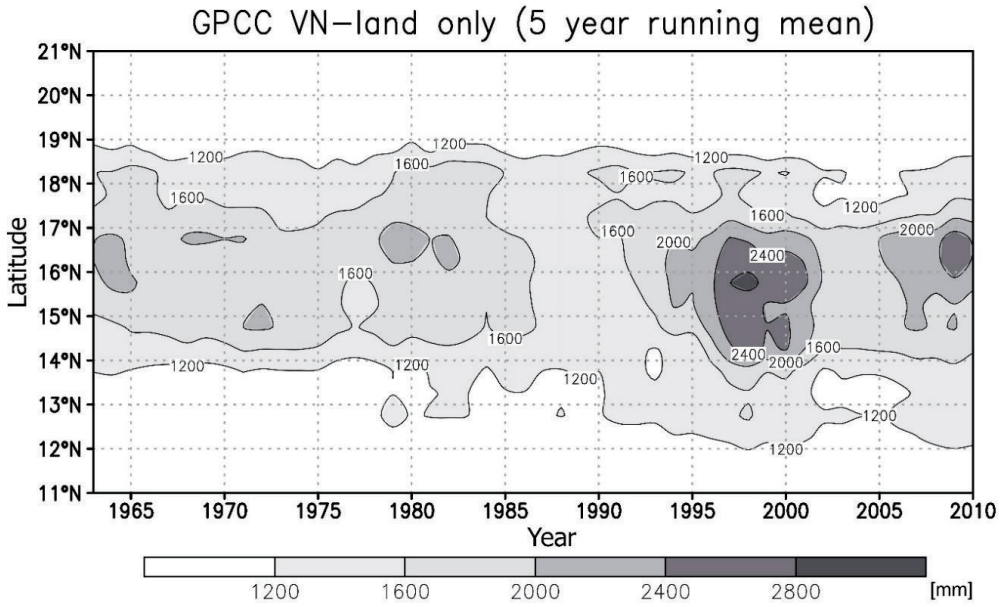

Fig. 3 Five-year running mean of latitudinal mean GPCC SOND rainfall (Vietnam land only) from 1963 to 2010.

Figure 4 represents the inter-annual variations of SOND rainfall anomaly calculated by values from all the stations in the NR and SR. Both the average values and year-to-year variations of SOND rainfall in the SR (average=1176 mm) are relatively large compared to those in the NR (average=650 mm). As illustrated in Fig. 4a, the long-term trends of rainfall between the north and the south of Vietnam are noticeably different. In the NR, it is obvious that the rainfall amount has decreased since the late 1980s. Meanwhile, it tends to increase significantly (19.6 mm decade^{-1}) in the SR. In particular, the SR shows a 10.6% increase in rainfall in the period 1987–2012 (Epoch 2; E2) compared with 1961–1986 (Epoch 1; E1).

To consider the rainfall owing to synoptic scale systems, we computed the contribution of TCs (hereinafter, TC rainfall) and non-TC rainfall to SOND rainfall trends. This TC rainfall computation was based on Nguyen-Thi *et al.* (2012a), who assigned rainfall induced by TC if the TC center is located within 600 km from the station. In regional scales, TC rainfall contributed approximately6.2% and 10.3% to the total SOND rainfall in the NR and SR, respectively. Figure 4b shows that the SOND TC rainfall in the SR has increased during the period 1961–2012, which is consistent with the findings of Nguyen-Thi *et al.* (2012b), who also reported significant increasing

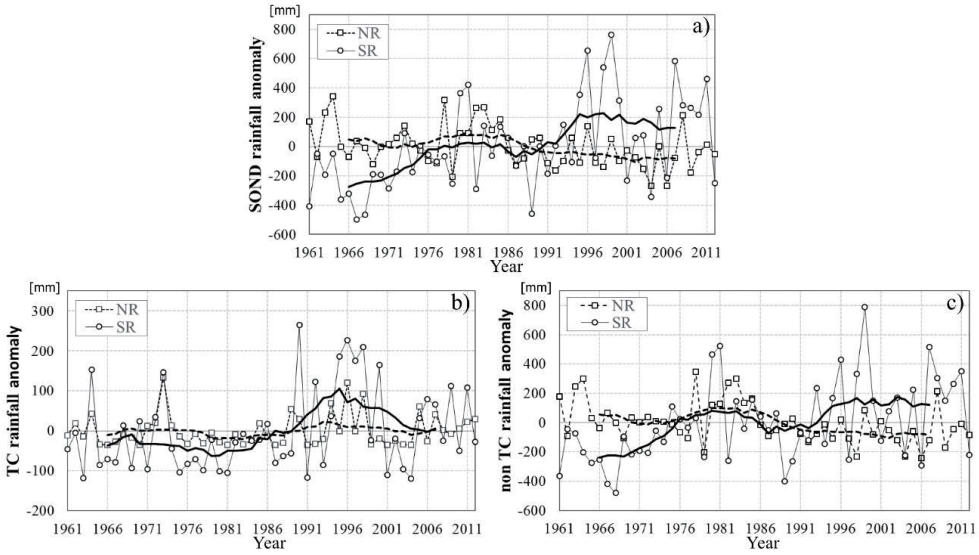

Fig. 4 Inter-annual variations of SOND rainfall anomaly in the NR (broken line) and SR (solid line) for (a) station-averaged rainfall (b) TC rainfall and (c) non-TC rainfall. Thick lines show their 11-year running mean.

trends of TC rainfall amounts as well as TC heavy rainfall days. Simultaneously, non-TC rainfall in the SR, which might be due to ITCZ, the northeast monsoon, or local convective systems, also shows an increasing trend (Fig. 4c). It is worth noting that TC rainfall in E2 is ~55% larger than that in E1 over the SR. This analysis confirms that not only TC rainfall but also non-TC rainfall have increased significantly (7.9 mm decade^{-1} and 11.7 mm decade^{-1} respectively) over the SR.

4. Rainfall Change Associated with Dynamics and Thermodynamics of Large-scale Circulation Features

The 52-year climatology of 850 hPa winds for SOND (Fig. 5a) shows northeasterlies associated with northeast monsoon over SR and easterlies over NR of Vietnam. These strong northeasterlies strike the windward side of the Truong Son mountain range (Fig. 1a) over central Vietnam, and therefore create a higher potential for an orographic-forced mechanism towards the windward side. In the windward side of the Truong Son mountain range, strong convergence and continuum of wind velocity are prominent. The amount of kinetic energy accumulations over the region would be high enough to force the orographic mechanism, which could contribute to precipitation in the presence of higher moisture transport and moisture flux convergence, and accumulation over the region owing to northeasterlies, as shown in Fig. 5b. The climatology of wind and moisture dynamics clearly shows that most of the moisture for the precipitation over the central and south region is contributed by northeasterlies.

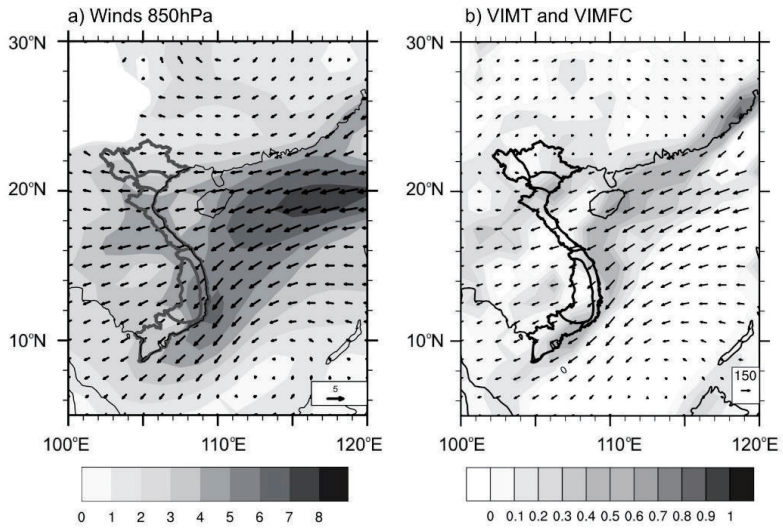

Fig. 5 The 1961–2012 SOND climatology of (a) 850 hPa winds (vector; m s^{-1}), and wind speed (shading; m s^{-1}), b) Vertically integrated moisture flux transport (vector; kg m^{-1} s^{-1}) and vertically integrated moisture flux convergence (shading; kg kg^{-1} s^{-1}). The missing values denote where the pressure surface is lower than topography.

Figure 6 shows the 52-year SOND trend of wind, SST, evaporation, specific humidity at 2 m, VIMFC, and OLR. The long-term trend of SOND wind field at 850 hPa (Fig. 6a) shows the significant enhancement in northeasterly winds over the VES predominantly over the south of the VES (11–16°N; 109–115°E; SVES), with westerly winds strengthened over the SR. The northeasterly wind trend is significant on the eastern coast of central Vietnam reflecting the strengthening of the northeast monsoon. In the SR, westerly/southwesterly wind trends are dominant. The strengthening of these two prominent wind patterns over SVES would be an important factor for the increasing trends of Pav and R50mm rainfall over the central and SR.

Figure 6a shows the SOND SST trend over the VES for the period from 1961–2012. The SST over the SVES exhibits a significant warming of 0.8–1.2 °C for the 52-year period. Meanwhile, the SST increasing trend is rather small and not significant over the NVES. The warming over the SVES is part of the western Pacific warming, which induces changes in large-scale circulations, and might thus affect the northeast monsoon by strengthening the northeasterly winds. Over the NVES, as SST and 850 hPa winds do not show any significant trend, the NVES region is excluded from the analysis. A correlation exists between the 52-year SOND rainfall amount over Vietnam and the SST over the SVES (not shown), indicating a positive and negative relationship with rainfall over the SR and NR, respectively. As a consequence, the rainfall increase over the SR is associated to the warming over the SVES.

Further investigation was performed to assess the VES warming and its association with rainfall increase over the SR by considering the dynamics and thermodynamics of large-scale circulation features. Figure 6b shows a significant increasing trend of evaporation over the SVES. According

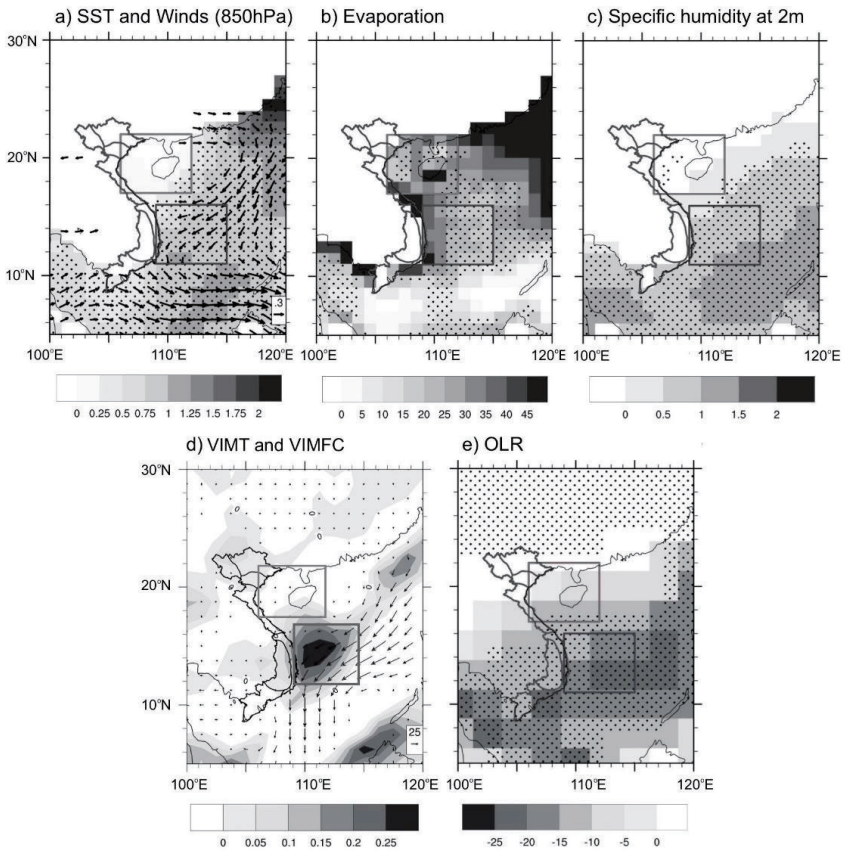

Fig. 6 Long-term SOND trends for (a) 850 hPa wind (vector) and SST (shading), (b) evaporation (mm), c) specific humidity at 2 m (g kg^{-1}), d) vertically integrated moisture flux transport (vector; kg m^{-1} s^{-1}) and convergence (shading; kg kg^{-1} s^{-1}), and e) outgoing longwave radiation (W m^{-2}). The dotted region denotes statistical significance at the 5% level. In case of vectors, only significant vectors at 5% level are shown. Rectangular boxes show north and south VES, respectively.

to the Clausius–Clapeyron rate, approximately 1 °C warming of the VES should be able to hold ~7% more specific humidity (Trenberth *et al*. 2003). Therefore, a significantly higher evaporation of approximately 10–20 mm over the VES results in greater moisture availability, especially over the SVES, as confirmed from the significant increasing trend of specific humidity over most parts of the VES in the last 52 years (Fig. 6c). Increase in humidity, along with strengthening of the northeasterlies over the VES caused more moisture over the SR. Additionally, the increasing trend of VIMFC and the transport of VIMT support the increase in moisture convergence accumulation, that enhance heavy rainfall over the eastern coast of central Vietnam and the SR (Fig. 6d).

The primary moisture transport over SVES is due to the northeast monsoon flow. Yokoi and Matsumoto (2008) demonstrated that northerly and southerly wind anomalies play a very important role in the heavy rainfall over the SR. The long-term trends of wind anomalies in the lower atmosphere of the VIMFC and VIMT confirm the strengthening of northeasterly winds and

moisture transport. Consequently, the VES warming (particularly over the SVES) has increased the moisture availability and strengthened the southwestward VIMT transport, thus resulting in a deeper convection over the SR and its adjacent SVES. To demonstrate deep convection, we used the OLR (Fig. 6e), where its negative trend (1974–2012) indicates the further deepening of convection and precipitating systems.

Li *et al.* (2015) and Nguyen-Le *et al.* (2015) reported that after the 1990s, tropical western Pacific warming and eastern Pacific cooling modulated the Walker circulation in a grand La Niña-like pattern (Xiang and Wang 2013). The La Niña-like pattern appears to control the background mean states of the SST and the circulation over the VES and western North Pacific. Such a change in the large-scale circulation, along with the warming of the SVES, wind circulation and northeast monsoon have significantly intensified and strengthened. The warming of the SVES and the circulation changes consequently affect the rainfall amount and the PIs over the SR.

5. Conclusions

In this study, the long-term changes of SOND rainfall over Vietnam for the period 1961–2012 were investigated. The 52-year rainfall trend indicated an obvious decrease/increase contrast to the north/south of 17°N in the coastal area of Vietnam. We also found that the increase in TC rainfall and non-TC rainfall contributed to the increase in rainfall amount over the SR. Moreover, similar rainfall trends were found in the PIs such as Rx1day and R50mm.

The increasing trend of SOND rainfall in the last 52 years was found to be linked to the changes in the SST over the SVES. This type of inter-annual autumn rainfall variations could be associated with the dominant La Niña-like pattern, which might alter large-scale circulations. The warming of the SVES resulted in the increase in the evaporation and 2-m specific humidity over the SVES. The added availability of moisture along with the strengthening of the northeasterly contributed to the moisture convergence over the SR, resulting in an increase in the deep convection over the SR. Our findings and analysis indicated that the inter-annual variation of SOND rainfall over Vietnam was associated with the local VES SST variations along with the La Niña-like pattern. Therefore, a proper representation of the SST as the lower boundary condition in the regional climate models could clarify the inter-annual variation of SOND rainfall over Vietnam. Thus, the relationship sensitivity between the SOND rainfall of Vietnam and the SST over the VES should be considered in a future study.

Acknowledgments

Long Trinh-Tuan and Rakesh Teja Konduru are supported by the Tokyo Human Resources Fund for City Diplomacy from the Tokyo Metropolitan Government, Japan. Thanh Ngo-Duc is supported by the Vietnam National Foundation for Science and Technology Development (NAFOSTED) under Grant 105.06-2018.05. Jun Matsumoto was supported by the Grant-in-Aid for Scientific Research No. 26220202. We appreciate valuable comments and suggestions by Prof. Hideo Takahashi, Prof. Hiroshi Matsuyama, and Dr. Daisuke Ishimura, Department of Geography, Tokyo Metropolitan University. We thank VNMHA for providing the rain gauge data. The JTWC best

track data were sourced from http://www.metoc.navy.mil/jtwc. The HadISST data were retrieved from https://climatedataguide.ucar.edu/climate-data/sst-data-hadisst-v11.

Reference

Banacos, P. C., and Schultz, D. M. 2005. The use of moisture flux convergence in forecasting convective initiation: Historical and operational perspectives. *Wea. Forecasting* **20**: 351–366.

Chen, T. C., Tsay, J. D., Yen, M. C., and Matsumoto, J. 2012. Interannual variation of the late fall rainfall in central Vietnam. *J. Climate* **25**: 392–413.

Chen, T. C., Matsumoto, J., and Alpert, J. 2015a. Development and formation mechanism of the Southeast Asian winter heavy rainfall events around the South China Sea. Part I: Formation and propagation of cold surge vortex. *J. Climate* **28**: 1417–1443.

Chen, T. C., Matsumoto, J., and Alpert, J. 2015b. Development and formation mechanism of the Southeast Asian winter heavy rainfall events around the South China Sea. Part II: Multiple interactions. *J. Climate* **28**: 1444–1464.

Endo, N., Matsumoto, J., and Lwin, T. 2009. Trends in precipitation extremes over Southeast Asia. *SOLA* **5**: 168–171.

Granato, G. E. 2006. Kendall–Theil Robust Line (KTRLine, version 1.0). *Techniques and Methods of the US Geological Survey*, 31.

Kendall, M. G. 1975: *Rank Correlation Methods,* Griffin, London

Kobayashi, C., Endo, H., Ota, Y., Kobayashi, S., Onoda, H., Harada, Y., Onogi, K., and Kamahori, H. 2014. Preliminary results of the JRA-55C, an atmospheric reanalysis assimilating conventional observations only. *SOLA* **10**: 78–82.

Kobayashi, S., Ota, Y., Harada, Y., Ebita, A., Moriya, M., Onoda, H., Onogi, K., Kamahori, H., Kobayashi, C., Endo, H., Miyaoka, K., and Takahashi, K. 2015. The JRA-55 reanalysis: General specifications and basic characteristics. *J. Met. Soc. Japan* **93**: 5–48.

Lee, H. T. 2014. Climate algorithm theoretical basis document (C-ATBD): Outgoing longwave radiation (OLR)—Daily. NOAA's Climate Data Record (CDR) Program. *Technical Report CDRP-ATBD-0526*.

Li, T., Zhang, L., and Murakami, H. 2015. Strengthening of the Walker circulation under global warming in an aqua-planet general circulation model simulation. *Adv. Atmos. Sci.* **32**: 1473–1480.

Matsumoto, J. 1997. Seasonal transition of summer rainy season over Indochina and adjacent monsoon region. *Adv. Atmos. Sci.* **14**: 231–245.

Matsumoto, J., Wang, B., Wu, G., Li, J., Wu, P., Hattori, M., Mori, S., Yamanaka, M., Ogino, S., Hamada, J-I., H., Syamsudin, F., Koike, T., Tamagawa, K., Ikoma, E., Kinutani, H., Kamahori, H., Kamiguchi, K., and Harada, Y. 2017. An overview of the Asian Monsoon Years 2007–2012 (AMY) and multi-scale interactions in the extreme rainfall events over the Indonesian maritime continent. In *The Global Monsoon System: Research and Forecast, 3rd,* eds. Chang, C. P., Kuo, H. C., Lau, N. C., Johnson, R. H., Wang, B., and Wheeler, M. 365–385, World Scientific.

Nguyen-Le, D., Matsumoto, J., and Ngo-Duc, T. 2015. Onset of the rainy seasons in the eastern Indochina Peninsula. *J. Climate* **28**: 5645–5666.

Nguyen-Le, D., and Matsumoto, J. 2016. Delayed withdrawal of the autumn rainy season over central Vietnam in recent decades. *Int. J. Climatol*. **36**: 3002–3019.

Nguyen-Thi, H. A., Matsumoto, J., Ngo-Duc, T., and Endo, N. 2012a. A climatological study of tropical cyclone rainfall in Vietnam. *SOLA* **8**: 41–44.

Nguyen-Thi, H. A., Matsumoto, J., Ngo-Duc, T., and Endo, N. 2012b. Long-term trends in tropical cyclone rainfall in Vietnam. *J. Agrofor. Environ.* **6**: 89–92.

Nguyen-Xuan, T., Ngo-Duc, T., Kamimera, H., Trinh-Tuan, L., Matsumoto, J., Inoue, T., and Phan-Van, T. 2016. The Vietnam Gridded Precipitation (VnGP) Dataset: Construction and Validation. *SOLA* **12**: 291–296.

Phan, V. T., Ngo-Duc, T., and Ho, T. M. H. 2009. Seasonal and interannual variations of surface climate elements over Vietnam. *Clim. Res*. **40**: 49–60.

Rayner, N. A., Parker, D. E., Horton, E. B., Folland, C. K., Alexander, L. V., Rowell, D. P., Ken E. C., and Kaplan, A. 2003. Global analyses of sea surface temperature, sea ice, and night marine air temperature since the late nineteenth century. *J. Geophys. Res*. **108**: (D14) 4407.

Schneider, U., Becker, A., Finger, P., Meyer-Christoffer, A., and Rudolf, B. 2015. GPCC Full Data Reanalysis Version 7.0 at 0.5°: Monthly Land-Surface Precipitation from Rain-Gauges built on GTS-based and Historic Data. doi:10.5676/DWD_GPCC/FD_M_V7_050

Sen, P. K. 1968. Estimates of the regression coefficient based on Kendall's tau. *J. Am. Stat. Assoc* **63**: 1379–1389.

Trenberth, K. E., Dai, A., Rasmussen, R. M., and Parsons, D. B. 2003. The changing character of precipitation. *Bull. Amer. Met. Soc.* **84**: 1205–1217.

Villafuerte II, M. Q., and Matsumoto, J. 2015. Significant influences of global mean temperature and ENSO on extreme rainfall in Southeast Asia. *J. Climate* **28**: 1905–1919.

Wu, P., Fukutomi, Y., and Matsumoto, J. 2012. The impact of intraseasonal oscillations in the tropical atmosphere on the formation of extreme central Vietnam precipitation. *SOLA* **8**: 57–60.

Xiang, B., and Wang, B. 2013. Mechanisms for the advanced Asian summer monsoon onset since the mid-to-late 1990s. *J. Climate* **26**: 1993–2009.

Yatagai, A., Kamiguchi, K., Arakawa, O., Hamada, A., Yasutomi, N., and Kitoh, A. 2012. APHRODITE: Constructing a long-term daily gridded precipitation dataset for Asia based on a dense network of rain gauges. *Bull. Amer. Met. Soc.* **93**: 1401–1415.

Yen, M. C., Chen, T. C., Hu, H. L., Tzeng, R. Y., Dinh, D. T., Nguyen, T. T. T., and Wong, C. 2011. Interannual variation of the fall rainfall in Central Vietnam. *J. Met. Soc. Japan* **89**: 259–270.

Yokoi, S., and Matsumoto, J. 2008: Collaborative effects of cold surge and tropical depression–type disturbance on heavy rainfall in central Vietnam. *Mon. Wea. Rev.* **136**: 3275–3287.